ARTICLE IN PRESS

Available online at www.sciencedirect.com

SCIENCE DIRECT®

Journal of Electroanalytical Chemistry xxx (2003) xxx–xxx

Journal of Electroanalytical Chemistry

www.elsevier.com/locate/jelechem

Study of the effect of the membrane composition on ion transfer across a supported liquid membrane

Lasse Murtomäki [a,*], Michael H. Barker [a,1], José A. Manzanares [b], Kyösti Kontturi [a]

[a] *Laboratory of Physical Chemistry and Electrochemistry, Helsinki University of Technology, P.O. Box 6100, FIN-02015 HUT, Finland*
[b] *Department of Thermodynamics, Faculty of Physics, University of Valencia, 46100 Burjassot, Spain*

Received 3 April 2003; received in revised form 23 June 2003; accepted 29 June 2003

Abstract

The rate of ion transfer across the supported liquid membrane (SLM) is studied in the rotating diffusion cell (RDC), varying the chemical composition of the SLM from net-cloth supported gel membranes to radiation-grafted polymer membranes. Steady-state current–voltage curves are measured as a function of the rotation rate, and values for the standard rate constant, k^0, are determined for a series of tetraalkylammonium cations from the analysis of the initial slopes and the diffusion limiting currents. The analysis gives values for k^0 of the order of 10^{-2}–10^{-4} cm s^{-1}, which is in rather good agreement with the values found in the literature for this type of the system. As controlled delivery of ionic drugs can be achieved by control of the electric current, whereby the SLM acts as a drug reservoir, the study is extended to the release of the anti-Alzheimer drug Tacrine, where ion-exchange fibers are embedded in the membrane as the drug carrier. Our previous transient experiments are also discussed, and it is suggested that their interpretation is seriously hampered by the non-uniform potential distribution, which brings about high capacitive currents.

Keywords: Supported liquid membrane; Controlled drug delivery; Ion transfer kinetics

1. Introduction

A supported liquid membrane, SLM, is usually formed by impregnating a non-volatile organic solvent into an inert and porous polymer membrane, whereby the solvent is held within the membrane by capillary forces. Placing the SLM between two aqueous solutions, a heterogeneous system is brought about, which can be applied in, e.g., hydrometallurgy [1], waste solvent treatment and electrochemical sensor applications [2] or biomembrane studies. A SLM thus has two aqueous/organic interfaces through which mass transfer can take place, subject to restrictions characteristic to the problem, such as mass balance or electroneutrality.

We have previously used SLMs in a rotating diffusion cell [3] as a means to study ion transfer kinetics across the aqueous/organic interface. Surprisingly, both steady state [4] and transient [5] measurements resulted in unpredictably low (of the order of 10^{-4} cm s^{-1}) values of the standard rate constants of ion transfer according to the Butler–Volmer formalism, when compared with the results obtained at a single interface. Furthermore, the peak currents in cyclic voltammograms were significantly higher than predicted by the usual Nicholson–Shain formula. We could not give any explanation for these findings but could only speculate about some yet unidentified membrane or solvent effects [6].

In this communication, we address these dilemmas afresh, and study the role of the membrane in a more versatile manner. This is accomplished by varying the support of the membrane from an ordinary net-cloth to radiation-grafted polymers [7,8], as well as the chemical composition of the membrane. The further motivation of our work is an interesting pharmaceutical application, where the compound to be delivered is initially bound to a gel-patch, and upon application of an elec-

* Corresponding author. Tel.: +358-9-4512575; fax: +358-9-4512580.
E-mail address: lasse.murtomaki@hut.fi (L. Murtomäki).
[1] Present address: Outokumpu Research Oy, P.O. Box 60, FIN-28101 Pori, Finland.

0022-0728/$ - see front matter © 2003 Elsevier B.V. All rights reserved.
doi:10.1016/j.jelechem.2003.06.010

tric current it is released from the patch in a controlled manner. These types of devices are assigned to long-term delivery for patients who are necessarily not able to monitor drug intake by themselves [9]. We use a rather lipophilic anti-Alzheimer drug Tacrine as a probe, and study its release kinetics from a membrane phase gelled with PVC and including an ion-exchange fiber as the initial drug carrier.

2. Theory

We adopt here the Butler–Volmer formalism for the ion transfer kinetics, recognizing that it is just a phenomenological approach; this question has been widely discussed in the literature, and we are not going to repeat it. The only aspect of the Butler–Volmer approach that we consider here is that we concentrate on the analysis at low overpotentials where the linearisation can be carried out. The reason is that there is no a priori knowledge of the value of the charge transfer coefficient α at high overpotentials, but in the vicinity of zero its value has been shown to be 1/2 regardless of the theoretical approached adopted [10,11]. Its meaning in the case of ion transfer is also a little unclear, although the description that it reflects the relative portions of the potential drops in the double (or possible inner) layers is most plausible [12].

We repeat only the main features of the transport equations to make the paper more readable. From our previous paper [5] the current-overpotential equation is obtained as

$$\begin{aligned}\frac{I}{I_0} &= \frac{c^{\mathrm{w}}(0)}{c_{\mathrm{b}}^{\mathrm{w}}}\mathrm{e}^{-\alpha f\eta_1} - \frac{c^{\mathrm{o}}(0)}{c_{\mathrm{b}}^{\mathrm{o}}}\mathrm{e}^{(1-\alpha)f\eta_1} \quad \text{left boundary } x=0,\\ \frac{I}{I_0} &= \frac{c^{\mathrm{o}}(h)}{c_{\mathrm{b}}^{\mathrm{o}}}\mathrm{e}^{(\alpha-1)f\eta_2} - \frac{c^{\mathrm{w}}(h)}{c_{\mathrm{b}}^{\mathrm{w}}}\mathrm{e}^{\alpha f\eta_2} \quad \text{right boundary } x=h.\end{aligned} \tag{1}$$

In Eq. (1), I is the current, I_0 is the exchange current, h is the membrane thickness and $f = F/RT$, where F, R and T have their usual significance. $c^{\mathrm{w,o}}(0,h)$ and $c_{\mathrm{b}}^{\mathrm{w,o}}$ are the surface and bulk concentrations of the transferring ion: the superscript 'w' or 'o' indicates the water or the organic (membrane) phase. The overpotentials η_1 and η_2 are defined as $\eta_{1,2} = \Delta\phi_{1,2} - \Delta\phi_{1,2}^{\mathrm{eq}}$, where $\Delta\phi_1 = \phi^{\mathrm{o}}(0) - \phi^{\mathrm{w}}(0)$ and $\Delta\phi_2 = \phi^{\mathrm{w}}(h) - \phi^{\mathrm{o}}(h)$, and ϕ is the Galvani potential. From these definitions, it follows that $\Delta\phi_1^{\mathrm{eq}} = -\Delta\phi_2^{\mathrm{eq}}$, and consequently, $\Delta\phi_1 + \Delta\phi_2 = \eta_1 + \eta_2$.

The exchange current I_0 is given as

$$I_0 = AFk^0\left(c_{\mathrm{b}}^{\mathrm{w}}\right)^{1-\alpha}\left(c_{\mathrm{b}}^{\mathrm{o}}\right)^{\alpha}, \tag{2}$$

where A is the interfacial area and k^0 the standard rate constant of ion transfer according to the Butler–Volmer formalism. Close to the equilibrium ($\eta_{1,2} = 0$, $I = 0$, $c^{\mathrm{w,o}}(0) = c^{\mathrm{w,o}}(h) = c_{\mathrm{b}}^{\mathrm{w,o}}$) Eq. (1) can be linearized to give

$$\begin{aligned}\frac{I}{I_0} &= \frac{c^{\mathrm{w}}(0)}{c_{\mathrm{b}}^{\mathrm{w}}} - \frac{c^{\mathrm{o}}(0)}{c_{\mathrm{b}}^{\mathrm{o}}} - f\eta_1,\\ \frac{I}{I_0} &= \frac{c^{\mathrm{o}}(h)}{c_{\mathrm{b}}^{\mathrm{o}}} - \frac{c^{\mathrm{w}}(h)}{c_{\mathrm{b}}^{\mathrm{w}}} - f\eta_2.\end{aligned} \tag{3}$$

The surface concentrations $c^{\mathrm{o,w}}(0)$ and $c^{\mathrm{o,w}}(h)$ can be expressed in terms of the current, and Eq. (3) becomes

$$\begin{aligned}\frac{I}{I_0} &= \left(1 - \frac{I}{I_{\mathrm{L}}^{\mathrm{w}}}\right) - \left(1 + \frac{I}{I_{\mathrm{L}}^{\mathrm{o}}}\right) - f\eta_1 = -\frac{I}{I_{\mathrm{L}}^{\mathrm{w}}} - \frac{I}{I_{\mathrm{L}}^{\mathrm{o}}} - f\eta_1,\\ \frac{I}{I_0} &= \left(1 - \frac{I}{I_{\mathrm{L}}^{\mathrm{o}}}\right) - \left(1 + \frac{I}{I_{\mathrm{L}}^{\mathrm{w}}}\right) - f\eta_2 = -\frac{I}{I_{\mathrm{L}}^{\mathrm{w}}} - \frac{I}{I_{\mathrm{L}}^{\mathrm{o}}} - f\eta_2\end{aligned} \tag{4}$$

from which it is immediately seen that $\eta_1 = \eta_2$. $I_{\mathrm{L}}^{\mathrm{w,o}}$ is the limiting current in the appropriate phase, given by [4,13]

$$\begin{aligned}I_{\mathrm{L}}^{\mathrm{w}} &= 0.620FA(D^{\mathrm{w}})^{2/3}\nu^{-1/6}\omega^{1/2}/2c_{\mathrm{b}}^{\mathrm{w}},\\ I_{\mathrm{L}}^{\mathrm{o}} &= 4FAD^{\mathrm{o}}c_{\mathrm{b}}^{\mathrm{o}}/h,\end{aligned} \tag{5}$$

where ν is the kinematic viscosity of the aqueous phase (ca. 0.01 $\mathrm{cm^2\,s^{-1}}$), ω the angular frequency; $D^{\mathrm{w,o}}$ is the diffusion coefficient in the appropriate phase. The potential drop across the membrane can easily be solved as

$$\begin{aligned}\Delta\phi_{\mathrm{m}} &= \frac{RT}{F}\ln\left(\frac{c^{\mathrm{o}}(h)}{c^{\mathrm{o}}(0)}\right) = \frac{RT}{F}\ln\left(\frac{1 - I/I_{\mathrm{L}}^{\mathrm{o}}}{1 + I/I_{\mathrm{L}}^{\mathrm{o}}}\right)\\ &= -\frac{2RT}{F}\operatorname{arctanh}\left(\frac{I}{I_{\mathrm{L}}^{\mathrm{o}}}\right) \approx -\frac{2RT}{F}\frac{I}{I_{\mathrm{L}}^{\mathrm{o}}},\end{aligned} \tag{6}$$

where the linearisation is valid at low currents. We want to emphasize that the potential difference expressed by Eq. (6) does include both the dissipative part, i.e., the 'ohmic drop' and the reversible part, i.e., the diffusion potential (see Appendix).

Now, the cell potential E can be written in terms of the current:

$$\begin{aligned}E &= \Delta\phi_1 + \Delta\phi_2 + \Delta\phi_{\mathrm{m}} = \eta_1 + \eta_2 + \Delta\phi_{\mathrm{m}}\\ &= -\frac{2RT}{F}\left[\frac{I}{I_0} + \frac{I}{I_{\mathrm{L}}^{\mathrm{w}}} + 2\frac{I}{I_{\mathrm{L}}^{\mathrm{o}}}\right].\end{aligned} \tag{7}$$

The minus sign comes from our convention of the direction of the positive current. If we neglect the sign, the apparent resistance of the cell is given as

$$R = \frac{E}{I} = \frac{2RT}{F}\left[\frac{1}{I_0} + \frac{1}{I_{\mathrm{L}}^{\mathrm{w}}} + \frac{2}{I_{\mathrm{L}}^{\mathrm{o}}}\right]. \tag{8}$$

R is obtained from the linear portion of the current–voltage curve, i.e., in the vicinity of zero current/potential. Hence for a plot of R as a function of $I_{\mathrm{L}}^{\mathrm{w}^{-1}}$, viz, with a varying rotation rate, a straight line is obtained with the slope of 51.3 mV and an intercept of

$$R_\infty = \frac{2RT}{F}\left[\frac{1}{I_0} + \frac{2}{I_{\mathrm{L}}^{\mathrm{o}}}\right]. \tag{9}$$

After subtraction for $I_{\mathrm{L}}^{\mathrm{o}}$, the intercept gives I_0 and thus k^0, because close to equilibrium $\alpha = 1/2$. Alternatively,

comparing the intercepts from experiments with varying aqueous phase concentration, I_L^o can be determined separately, and the effective diffusion coefficient D^o evaluated.

3. Experimental

Thin gel SLMs can be cast for use in transient measurements. For RDC measurements, the gel is sufficiently strong to separate the two aqueous phases, but deflects into a hemisphere. Such gel SLMs are too flexible to retain a rigid interface during rotation; in order to cancel this deflection, the gel was supported on an inert cloth mesh.

The mesh selected was ordinary net cloth containing holes of diameter between 1 and 2 mm. The net support was not soluble in either of the solvents under consideration; it was prepared for use by boiling for 3 h in MilliQ water (changed once per h) to remove any salts or particulates from the material. The material was dried and cut into circles of 4 cm diameter for RDC use and 2 cm for transient experiments.

Ortho-nitrophenyloctylether, *o*-NPOE [37682-29-4], and *ortho*-nitrophenyloctylether, *o*-NPPE [39645-91-5] (Fluka), LiCl (Merck) and high molar mass polyvinyl chloride (PVC, Sigma) were used as supplied. The tetraalkylammonium chlorides (alkyl = methyl, ethyl, propyl, butyl, pentyl or hexyl; TMAC1, TEAC1, TPrACl, TBAC1, TPeACl or THACl) were all used as supplied (Sigma, Aldrich or Fluka). The organic phase base electrolytes were prepared by precipitation of a small volume of the aqueous solution of each tetraalkylammonium chloride with an acetone solution of lithium tetrakis(pentafluorophenyl)borate, $LiTPBF_{20}$ [2797-28-6] (Boulder Scientific, CO, USA) as previously described [5]. The model drug Tacrine (9-acridinamine) hydrochloride [1684-40-8], (Sigma) was used as supplied, and the $TPBF_{20}$ salt of Tacrine was made in a similar manner to the organic phase base electrolytes. The ion-exchange fiber material employed was Smopex®-102 poly(ethylene-*g*-styrenesulfonic acid) fiber (SmopTech Co., Finland).

The gel was cast using the following method: 0.5 ml *o*-NPOE ($d_4^{20} = 1.041$) were added to a borosilicate glass crucible containing a pre-weighed amount of base electrolyte, e.g., $TBATPBF_{20}$, giving a 15 mM concentration of supporting electrolyte. The electrolyte solution was warmed on a hot plate to around 80 °C then 0.05 g of PVC was added to give a 10% v/w solution. The PVC was allowed to swell and the mixture became opaque and crystalline. The temperature was increased slowly until the crystallinity disappeared leaving a clear, golden gel-solution at 100–120 °C.

A glass slide (ca. $8 \times 8 \times 0.7$ cm) was warmed on the hot plate whilst the gel was under preparation. A square PTFE gasket was cut from PTFE sheet (Vink, Finland) with an internal size of 4.5×4.5 cm and thickness 0.265 mm (internal volume approx 0.54 cm^3). The gasket was laid on the glass slide, which was removed from the hot plate. Approximately 0.35 cm^3 of warm gel was poured onto the warm slide inside the gasket. A pre-cut circle of net cloth (diameter 4 cm) was laid on the gel and a second glass slide of similar size to the first, but at room temperature, was laid on top of the gasket. The sandwich was g-clamped and allowed to cool. By sandwiching the gel and net between two glass slides, a disk of gel/net composite was formed, the thickness of which was defined by the PTFE gasket separating the two glass plates. The glass plates were stored in the dark and opened immediately prior to use. Excess gel was trimmed away from the edge of the net, leaving a circular disk, see Fig. 1.

Hydrophobic polyvinylidene fluoride (PVDF) membranes (GVHP, Millipore, MA, USA) with a dry thickness of 125 μm and a pore size of 0.22 μm were radiation-grafted with acrylic acid monomers as described in detail in [7]. The degree of grafting was 30 wt%, i.e., upon grafting, the mass of the membrane increased by 30%. A comparison with the non-grafted membrane was also carried out.

The experimental setup employed for RDC and voltammetric measurements has been described earlier [4,5]; the gel composite was loaded into the cell as before. The cell was from Oxford Electrodes, with two large area Ag|AgCl electrodes made in-house:

Ag|AgCl|*x* mM CatCl
+ 100 mM LiCl||10%PVC in NPOE
+ 15mM $CatTPBF_{20}$||*x* mM CatCl
+ 100 mM LiCl|AgCl|Ag.

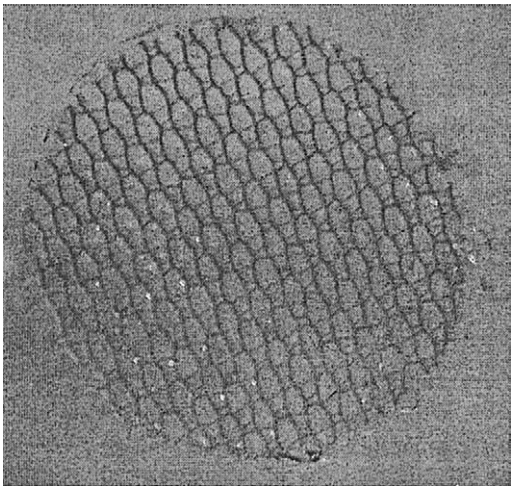

Fig. 1. A net-cloth supported NPOE–PVC gel membrane.

In this scheme 'Cat' denotes the probe cation used, viz tetraalkylammonium or Tacrine. The membrane was mounted in a PTFE holder so that a circular interface of 1 cm radius was exposed. The potentiostat was an Autolab PGSTAT100 (Ecochemie B.V., Netherlands [14]). Current–voltage curves were obtained by scanning the potential in the range $0 \rightarrow 0.3 \rightarrow -0.3 \rightarrow 0$ V at the rate of 1 mV s^{-1}. The rotation speed of the cell was varied from 2 to 10 Hz.

Impedance measurements were made at the start and end of each experiment to confirm that the cell resistance was constant throughout. The impedance equipment comprised of a 1286 potentiostat and a 1255 frequency response analyzer (Solartron, UK [15]).

4. Results and discussion

4.1. Gel membranes with alkylammonium cations

In Fig. 2, current–voltage curves of the net-cloth supported *o*-NPOE gel membrane are displayed for three rotating speeds, 2, 6 and 10 Hz. It is remarkable that although the scan rate is only 1 mV s^{-1}, an extensive current hysteresis takes place, as highlighted in Fig. 3 where Eq. (5) is applied. Although the linear correlation between the limiting currents and the square root of the angular frequency is remarkably good, bias currents of the order of 2–3 μA are found. This is partly because the current values have been taken as an average of the forward scan limiting currents of the positive and negative branches (absolute values). If the offset were interpreted solely as a capacitive current, the capacitance of the membrane would be of the order of 650–950 μF cm^{-2}, which is not credible. Obviously, the offset is an experimental artefact, because rather a long

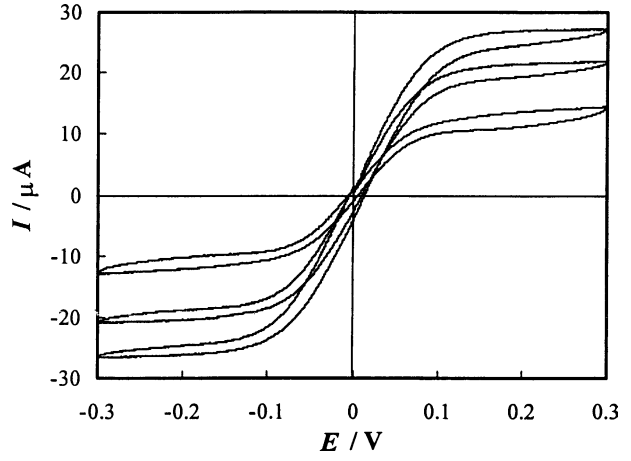

Fig. 2. Current–voltage curves of the net-cloth supported *o*-NPOE gel membrane at three rotating speeds, 2, 6 and 10 Hz. The common ion is TBA^+ at an aqueous concentration of 0.025 mM and a membrane concentration of 15 mM.

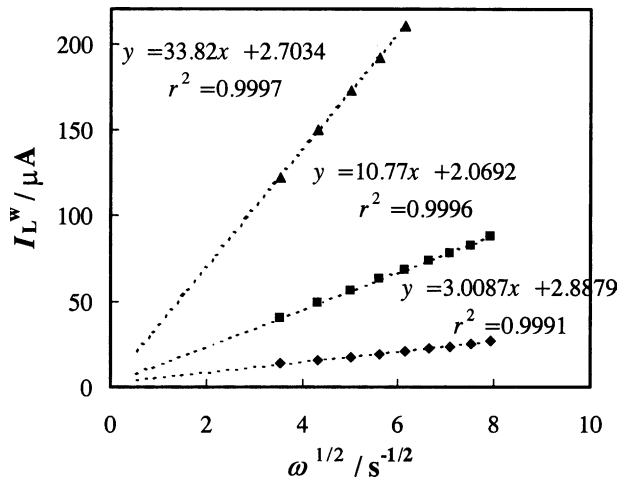

Fig. 3. Limiting currents of TBA^+ in the aqueous concentrations of 0.025 mM (◆), 0.1 mM (■) and 0.3 mM (▲).

time is required to bring the membrane back to its initial equilibrium state after a scan. Allowing the intercept to deviate from zero, the aqueous diffusion coefficient D^w can be evaluated from the slope as 4.7×10^{-6} cm^2 s^{-1} which compares well to a previously determined value of 5.9×10^{-6} cm^2 s^{-1} [4].

In Fig. 3, the limiting currents with 0.3 mM aqueous TBA^+ concentration are not displayed above the rotation frequency of 6 Hz because they level to ca. 215 μA. This apparently implies the change of the aqueous phase control to the membrane control. Using this current as an estimate of the limiting current in the membrane, I_L^o, the diffusion coefficient can be estimated as $D^o = 3.1 \times 10^{-7}$ cm^2 s^{-1} ($c_b^o = 15.0$ mM, $h = 265$ μm, $A = 3.14$ cm^2). This also is a credible number if compared to D^w and recalling Walden's rule of the viscosity ratios ($D^w/D^o \approx 14 \approx \eta^o/\eta^w$), or to the value reported by Samec et al. for TEA^+, 4.2×10^{-7} cm^2 s^{-1} [6].

The offset currents obtained from the linear fits in Fig. 3 were subtracted from the measured limiting currents, after which Eq. (8) was applied. The resistance values were deduced from the slopes of the *I–E* curves in the vicinity of the origin. In the case of 0.025 mM TBA^+ in the aqueous phases all the rotation frequencies were used in the analysis, while at the TBA^+ concentration of 0.1 mM the three highest, and at 0.3 mM all but the three lowest frequencies were rejected. The values of R of the rejected points leveled to a constant value, obviously reflecting the change to membrane phase control. The results are displayed in Fig. 4: the best result is obtained with the lowest aqueous concentration, where the slope almost coincides with the theoretical value 51.3 mV (= 51 300 μV).

From Eq. (9) it is seen that the intercepts of the straight lines of Fig. 4 provide the quantity R_∞ which is inversely proportional to the exchange current density and thus, in turn, to the square root of the aqueous

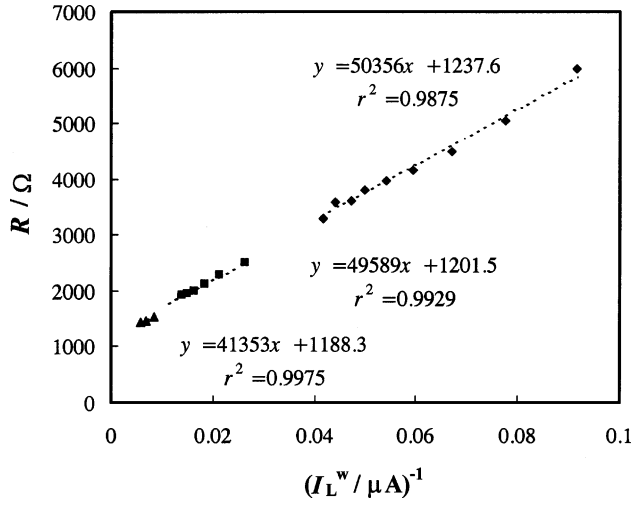

Fig. 4. The apparent resistance of the system according to Eq. (8). The symbols are as in Fig. 3.

phase concentration, Eq. (2). Despite the obvious inaccuracies of the values of R_∞ for the aqueous concentrations of 0.1 and 0.3 mM, a plot of R_∞ vs. $(c_b^w)^{-1/2}$ is displayed in Fig. 5. Again, the plot is quite good, and from the slope the standard rate constant k^0 is obtained as 3.94×10^{-3} cm s^{-1}. In conclusion, the value of the rate constant now is an order of magnitude higher than previously measured [4,5]; we believe that it is of the correct order of magnitude, although not very accurate.

From the intercept the limiting current in the membrane phase takes the value of 87.9 μA, which is, however, less than the measured limiting currents with $c_b^w = 0.3$ mM. In terms of resistance,

$$\frac{4RT}{F \times 87.9\ \mu A} \approx 1170\ \Omega \quad \text{and} \quad \frac{4RT}{F \times 215\ \mu A} \approx 480\ \Omega.$$

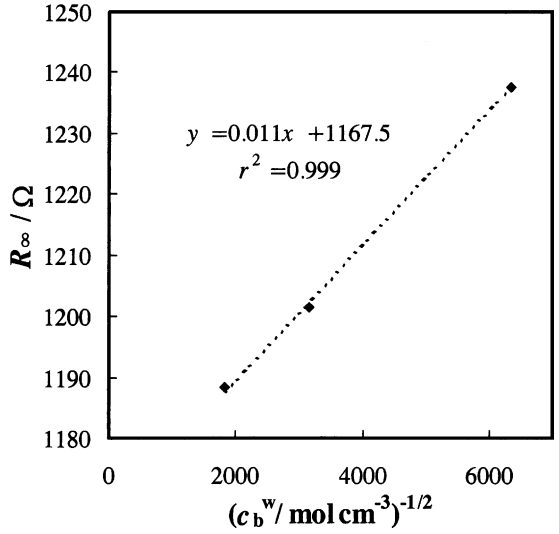

Fig. 5. The test of Eq. (9) for the three different concentrations of TBA^+.

Hence, an extra resistance of ca. 690 Ω resides in the cell. The conductivity of the aqueous supporting electrolyte, 100 mM LiCl, is ca. 10 mS cm^{-1}. To account for 690 Ω in the aqueous phase resistance, a cell constant (L/A) of ca. 6.9 cm^{-1} is required. The electrodes in the cell were located approximately 5 mm on either side of the membrane, making the cell constant ca. $2 \times (0.5\ \text{cm}/3.14\ \text{cm}^2) \approx 0.32\ \text{cm}^{-1}$, corresponding to 32 Ω. Thus, the ohmic resistance of the aqueous phases cannot entirely explain the extra resistance. In the Bode plot in Fig. 6, it is also seen that the cell resistance is, indeed, higher than expected, leveling to ca. 900 Ω. Where this resistance comes from, is still unclear to us; this is discussed later.

Next a series of tetraalkylammonium cations with varying alkyl chain length from methyl to hexyl was compared. It appeared that the potential window of the tetramethylammonium was too narrow to obtain a clearly defined limiting current, and it was left out of the analysis. Furthermore, recrystallisation of the tetrahexylammonium $TPBF_{20}$ salt after its metathesis was not successful, as it remained in an oily state in the solution. Hence, tetraethylammonium (TEA^+), tetrapropylammonium ($TPrA^+$), tetrabutylammonium (TBA^+) or tetrapentylammonium ($TPeA^+$) were added as a concentration of 15 mM to the membrane and 0.1 mM in the flanking aqueous phases.

From the plots I_L^w vs. $\sqrt{\omega}$ the aqueous diffusion coefficients D^w, shown in Table 1, were determined. Using the commonly preferred viscosity ratio 15 [16], the corresponding diffusion coefficients in the membrane phase, D^o, and consequently I_L^o were calculated. The resistances according to Eq. (8) were determined and plotted for each ion. As can be seen in Fig. 7, in all the cases the plots are rather good. The values of R_∞ were determined from the intercepts of the linear fits. The extra resistance $R_x = 690\ \Omega$ obtained above and the membrane resistance $R_m = 4RT/FI_L^o$ were subtracted from the values of R_∞, after which the charge transfer resistance $R_{ct} = 2RT/FI_0$ was available. From the charge transfer resistance the values k^0 in Table 1 were then calculated. Although this procedure admittedly is subject to some inaccuracy and

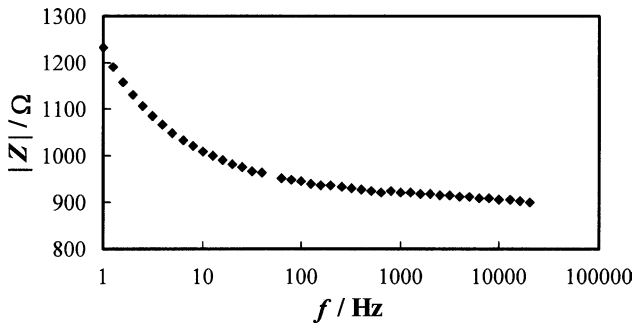

Fig. 6. Resistance of the cell, measured with ac impedance, prior to an experiment. The aqueous concentration of TBA^+ is 0.1 mM.

arbitrariness, it shows that reasonable values of kinetic parameters – at least of the proper order of magnitude – are achieved. The value of TEA^+, for example, is high enough that its cyclic voltammogram is practically indistinguishable from a voltammogram due to diffusion limited, i.e., reversible ion transfer.

4.2. Polymer membrane with and without grafting

Four different membrane compositions were studied varying the organic solvent from *o*-NPOE to *o*-NPPE, and taking the membrane with and without grafting. In all cases the probe cation was TBA^+ at a concentration of 15 mM in the membrane phase and 0.3 mM in the aqueous phases. The density of *o*-NPPE is $d_4^{20} = 1.098$, and its viscosity at 25 °C is 7.58 cP, much less than the value of *o*-NPOE at 25 °C, 12.35 cP [17]. The ratio $\eta^{\mathrm{NPPE}}/\eta^{\mathrm{NPOE}} \approx 0.6$ means that the membrane resistances R_m are related accordingly. Hence, if it is accepted that $R_\infty = R_x + R_\mathrm{ct} + R_\mathrm{m}$, it follows that

$$R_\infty^{\mathrm{NPOE}} - R_\infty^{\mathrm{NPPE}} = R_\mathrm{ct}^{\mathrm{NPOE}} - R_\mathrm{ct}^{\mathrm{NPPE}} + 0.4 \times R_\mathrm{m}^{\mathrm{NPOE}},$$

regardless of the value of R_x.

With the membranes without grafting the plots I_L^w vs. $\sqrt{\omega}$ gave for the aqueous diffusion coefficient of TBA^+, $D^\mathrm{w} = 4.3 \times 10^{-6}$ $\mathrm{cm^2\,s^{-1}}$, viz, practically the same as before. In the similar analysis as above, the following resistances were found:

- $R_\infty^{\mathrm{NPOE}} \approx 600\ \Omega$,
- $R_\infty^{\mathrm{NPPE}} \approx 500\ \Omega$.

In the gel membrane with a thickness of 265 μm, $R_\mathrm{m}^{\mathrm{NPOE}} = 480\ \Omega$. Assuming that the gel does not change the diffusion coefficient D^o significantly, as experiments also imply, it follows that in the GVHP membrane with a thickness of 125 μm, $R_\mathrm{m}^{\mathrm{NPOE}} = 125/265 \times 480\ \Omega \approx 230\ \Omega$, resulting in $R_\mathrm{ct}^{\mathrm{NPOE}} - R_\mathrm{ct}^{\mathrm{NPPE}} = 8\ \Omega$, which is of the order of the accuracy of our analysis. Hence, the change of the membrane solvent did not affect the release rate of the probe cation significantly. The same observation was made by Brown et al. [17], who studied carrier-mediated transport of alkali metal cations across a SLM impregnated with nitrophenyl alkyl ethers, varying the alkyl chains from C_2 to C_8. NPPE is, however, easier to handle, but more expensive.

When a grafted membrane impregnated with NPOE was used, the plot I_L^w vs. $\sqrt{\omega}$ gave $D^\mathrm{w} = 3.8 \times 10^{-6}$ $\mathrm{cm^2\,s^{-1}}$, which apparently reflects the fact that the active surface area of the membrane is ca. 87% of the geometrical area. Using this effective surface area correction, $R_\infty \approx 570\ \Omega$, slightly less than without grafting. It is difficult to make any closer comparison between the grafted and non-grafted membranes because grafting changes the structure of the polymer matrix so that the thickness, or merely the diffusion path length of the membrane becomes ambiguous.

A grafted membrane with *o*-NPPE did not show any clearly defined limiting current, which makes the further analysis impossible. Yet, plotting the current at any fixed potential as a function of $\sqrt{\omega}$ yielded a very nice straight line, the intercept of which was, however, as much as 45 μA. After the experiment it was seen that the solvent had redistributed from the center to the edges of the membrane. Grafting makes the membrane more hydrophilic because of the dissociating acrylic acid groups. This combined with the relatively low viscosity of NPPE apparently made the membrane hydrodynamically unstable.

Table 1
Data for the tetraalkylammonium and Tacrine cations in gel membranes

	TEA^+	$TPrA^+$	TBA^+	$TPeA^+$	$Tacrine^+$
$D^\mathrm{w}/10^{-6}$ $\mathrm{cm^2\,s^{-1}}$	6.9	5.1	4.4	3.5	4.7
$k^0/10^{-3}$ $\mathrm{cm\,s^{-1}}$	31.0	14.0	3.9	0.8	0.37[a]

[a] See Section 4.3

4.3. Release of Tacrine

In Tacrine studies, *o*-NPOE was used as the organic solvent, and the gel membrane was made without ion-exchange fiber and with 10 mg or 25 mg of fiber. The concentration of Tacrine was 15 mM in the membrane phase and 0.1 mM in the aqueous phases. With no fiber in the gel, a similar analysis as above for the alkylammonium cations gives for the standard rate constant, $k^0 = 3.7 \times 10^{-4}$ $\mathrm{cm\,s^{-1}}$, thus a very low value. This is contrasted by the previous finding by Mälkiä et al. [18] who, by applying ac voltammetry, obtained $k^0 > 0.1$ $\mathrm{cm\,s^{-1}}$, which corresponds to the case $R_\mathrm{ct} < 1\ \Omega$. They also found, using cyclic voltammetry, that for Tacrine, $D^\mathrm{w} = 7.3 \times 10^{-6}$ and $D^\mathrm{o} = 1.0 \times 10^{-7}$ $\mathrm{cm^2\,s^{-1}}$, which makes the ratio $D^\mathrm{w}/D^\mathrm{o} = 73$. The applicability of Walden's rule is thus questioned in the case of Tacrine, perhaps because it is not a spherical molecule, as can be seen from its molecular structure in Fig. 9. Using the viscosity ratio 15 along with the present value of D^w (see Table 1) gives $D^\mathrm{o} = 4.7/15 \times 10^{-6}$ $\mathrm{cm^2\,s^{-1}} = 3.1 \times 10^{-7}$ $\mathrm{cm^2\,s^{-1}}$.

Relying on the measured value $D^\mathrm{o} = 1.0 \times 10^{-7}$ $\mathrm{cm^2\,s^{-1}}$ [18], the membrane resistance is $R_\mathrm{m} = 1497\ \Omega$. From the present measurements it was found that $R_\infty = 1545\ \Omega$, making the charge transfer resistance $R_\mathrm{ct} = 48\ \Omega$, if the ambiguous $R_x = 690\ \Omega$ is ignored. This calculation leads to the value of $k^0 = 2.9 \times 10^{-3}$ $\mathrm{cm\,s^{-1}}$, which still is two orders of magnitude lower than that of Ref. [18]. If the aqueous phase resistances is taken to be 32 Ω, as discussed in paragraph 4.1, the charge transfer resistance is 12 Ω, corresponding to $k^0 = 0.012$ $\mathrm{cm\,s^{-1}}$. As our accuracy is of the order of 10 Ω , we cannot reach a better agreement with [18].

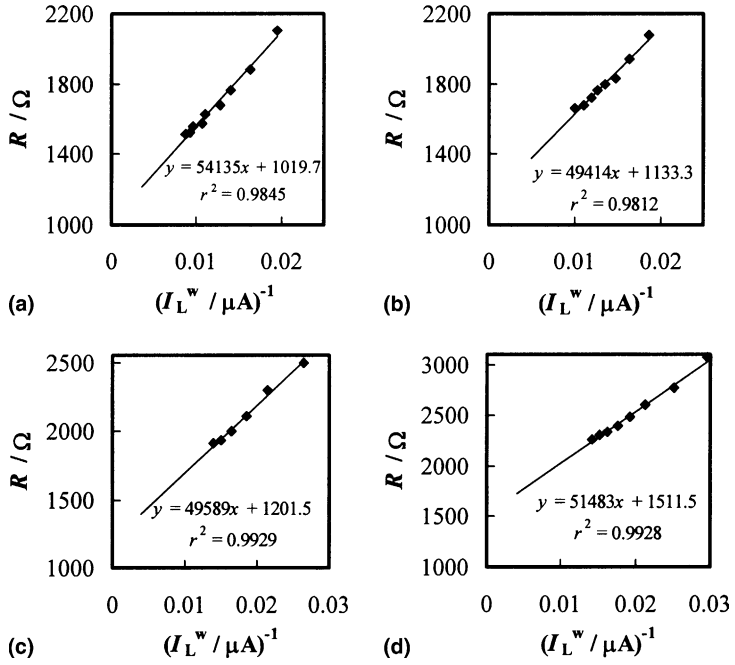

Fig. 7. Apparent resistance of the SLM with TEA^+ (a), $TPrA^+$ (b), TBA^+ (c) and $TPeA^+$ (d). Aqueous concentrations 0.1 mM and the membrane concentration 15 mM.

In Fig. 8, the limiting currents of Tacrine have been displayed. For the uppermost curve, with 25 mg of fiber added, there is no clearly defined current plateau, but the current values are read at 300 mV, where the other two systems reach the plateau. Again, similarly to the grafted membrane, quite a substantial offset current is observed. Apparently, by adding ion-exchange groups into the membrane phase, some other release mechanism is switched on. With no fiber in the membrane, $R_\infty \approx 1545\ \Omega$, and with 10 mg of fiber, $R_\infty \approx 1250\ \Omega$. This difference is expected as the rate of mass transport is enhanced due to the contribution of the ion- exchange mechanism within the membrane.

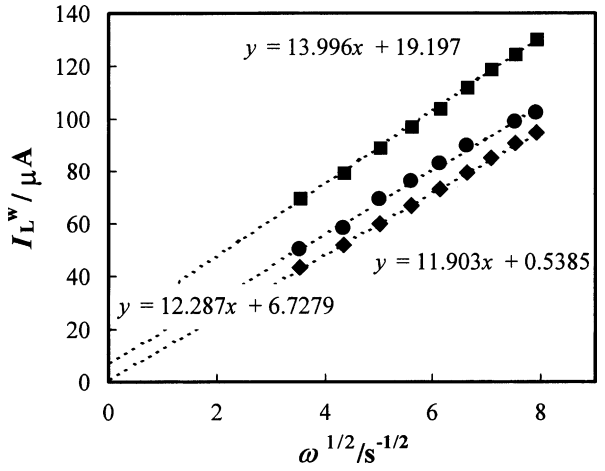

Fig. 8. Limiting currents of Tacrine in NPOE–PVC gel membranes: no fiber (◆), 10 mg of fiber (●) and 25 mg of fiber (■).

4.4. Extra resistance R_x

The mysterious extra resistance R_x requires a couple of comments. It has been suggested to us that it is the ohmic resistance of the membrane, which is not taken into account. As we show in Appendix, this is not quite the correct explanation. The Tacrine measurements discussed above imply that R_x could, however, reside in the membrane, i.e., the ionic mobilities are significantly lower than expected. Yet, the estimated membrane limiting current in the case of TBA^+ was in agreement with Walden's rule. In order to resolve this problem, experiments with low concentrations of the membrane phase electrolytes are needed, so that the membrane limiting current can be detected.

4.5. Transient experiments

In our previous paper [5], where cyclic voltammetry was carried out, the separation of the current peaks corroborated the result that the value of the standard

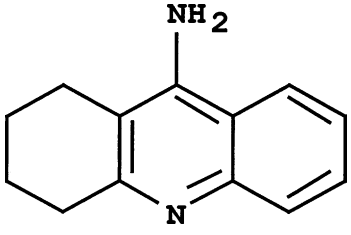

Fig. 9. Molecular structure of Tacrine.

rate constant k^0 would be of the order of 10^{-4} cm s^{-1}. The measured currents were, however, as much as 70% higher than simulated with $k^0 = 2 \times 10^{-4}$ cm s^{-1}. Yet, the limiting currents measured at steady state in a RDC [4] were in agreement with the Levich equation, Eq. (5). The question then arises, what is the fundamental difference between a transient and a steady-state experiment? The obvious answer is the capacitive current, but could it be that high? Now we think it could, based on the following reasoning:

As the electric current is continuous in an electroneutral system, the excess current, viz the capacitive current, is conducted across the membrane, increasing the ohmic drop within the membrane and the peak separation accordingly. From the simulation point of view, the value of k^0 has to be increased proportionally to keep the peak separation constant, which means an increase of the faradaic current. Hence, the difference between the measured current and the faradic current is less than 70%. A simulation for TBA^+ with $k^0 = 3.9 \times 10^{-3}$ cm s^{-1} determined above, at the scan rate of 75 mV s^{-1} gives a peak current ca. 43 μA while the measured current was ca. 60 μA. The difference, ca. 17 μA, would then correspond to the capacitance of ca. 290 μF cm^{-2} ($A = 0.785$ cm^2), which seems a little high at first glance, but it has to be recognized that almost the entire potential drop across the membrane is 'consumed' at that interface where the concentration polarisation takes place. In other words, the potential drop across the polarizing interface corresponds to the limit of the potential window in a single L|L electrochemical cell, as the measurements by Kihara and coworkers have shown [19]. The interfacial capacitance increases rapidly as the limits of the window are approached [20], and the value of 290 μF cm^{-2} is quite possible.

It can be argued that since the potential drop across the opposite interface is rather low, its capacitance is much lower, and in the series combination of two capacitors, only the lower of the two capacitances is observed:

$$C_T = \frac{C_1 C_2}{C_1 + C_2} \approx C_2 \quad \text{if } C_1 \gg C_2. \tag{10}$$

However, the situation cannot actually be described as the series combination of C_1 and C_2. The equivalent circuit of the membrane can be represented approximately as two parallel RC circuits in series plus the membrane resistance (written as $(R_1C_1)(R_2C_2)R_3$ with the notation of Autolab's fitting procedure). The separation of the resistive and reactive components from the total impedance is rather awkward, and does not clarify the situation at all, but the total capacitance of the membrane is not the issue in the first place. The gist is that at the polarizing interface both $\mathrm{d}\phi/\mathrm{d}t$ and the capacitance are high, creating a high capacitive current, which flows across the membrane. The capacitance of the interface is a function of the interfacial potential drop, and very difficult to estimate because the latter depends on the ohmic drop in the membrane and the other interface. A quantitative subtraction for the capacitive current requires knowledge of both the capacitance and $\mathrm{d}\phi/\mathrm{d}t$, which combined with the aforementioned problem of the charge transfer coefficient α, condemns the quantitative analysis of transient experiments to an unfortunate failure. Therefore, we are not going to analyze cyclic voltammograms any further.

5. Conclusions

The effect of the chemical composition on the rate of ion release from a supported liquid membrane, SLM, was studied. Previous results were critically reviewed, and it was found that an extra resistance resides somewhere in the rotating membrane cell. Correcting for this resistance, plausible values agreeing with the results obtained at the single liquid-liquid interface, are recovered. The release of probe ions from the SLM appears to be under mass transfer control, and the role of the membrane is of secondary importance, the only requirement being that the SLM is stable enough. The results of previous transient experiments with a SLM were discussed, at it is now believed that the several problems appearing in such experiments make the quantitative interpretation of them rather difficult.

Appendix A

The potential gradient in a system can be written in the general form of Eq. (A.1) [21]:

$$\nabla\phi = -\frac{j}{\kappa} - \frac{RT}{F}\sum_k \frac{t_k}{z_k}\nabla \ln c_k, \tag{A.1}$$

where ϕ is the Galvani potential, j is the current density, κ is the conductivity of the solution, t_k is the transport number, z_k is the charge number and c_k is the concentration of ion k; F, R and T have their usual significance. From Eq. (A.1), it is seen that the potential drop consists of two components: the dissipative term $-j/\kappa$, i.e., the ohmic drop, and the reversible term, i.e., the diffusion potential. Applying Eq. (A.1) in one dimension to the binary system, and integrating over the membrane, we obtain [21]:

$$\begin{aligned}\phi(h) - \phi(0) &= -j\int_0^h \frac{\mathrm{d}x}{\kappa} - \frac{(t_+ - t_-)RT}{F}\ln\frac{c(h)}{c(0)} \\ &= -j\int_0^h \frac{\mathrm{d}x}{\kappa} - \frac{D_+ - D_-}{D_+ + D_-}\frac{RT}{F}\ln\frac{c(h)}{c(0)},\end{aligned} \tag{A.2}$$

where $z_+ = -z_- = 1$, and $c_+ = c_- = c$. The conductivity of the solution is

$$\kappa(x) = \frac{F^2}{RT}(D_+ + D_-)c(x). \tag{A.3}$$

In order to calculate the integral in Eq. (A.2), the concentration profile $c(x)$ must be known. At steady state, according to our assumption, the anion is not moving because it cannot cross the membrane|solution interface. Therefore:

$$-J_- = D_-\left(\frac{\mathrm{d}c}{\mathrm{d}x} - \frac{F}{RT}c\frac{\mathrm{d}\phi}{\mathrm{d}x}\right) = 0 \;\Rightarrow\; \frac{\mathrm{d}c}{\mathrm{d}x} = \frac{F}{RT}c\frac{\mathrm{d}\phi}{\mathrm{d}x}, \tag{A.4}$$

where J_- is the flux density of the anion (mol $\mathrm{cm}^{-2}\,\mathrm{s}^{-1}$). Inserting this in to the Nernst–Planck equation of the cation, gives:

$$-J_+ = -\frac{j}{F} = D_+\left(\frac{\mathrm{d}c}{\mathrm{d}x} + \frac{F}{RT}c\frac{\mathrm{d}\phi}{\mathrm{d}x}\right) = 2D_+\frac{\mathrm{d}c}{\mathrm{d}x}. \tag{A.5}$$

Eq. (A.5) can readily be integrated:

$$c(x) = c(0) - \frac{j}{2D_+F}x. \tag{A.6}$$

The integral in Eq. (A.2) now becomes:

$$\begin{aligned} -j\int_0^h \frac{\mathrm{d}x}{\kappa} &= -j\frac{RT}{F^2(D_+ + D_-)}\int_0^h \frac{\mathrm{d}x}{c(x)} \\ &= +\frac{2D_+}{D_+ + D_-}\frac{RT}{F}\ln\frac{c(h)}{c(0)}. \end{aligned} \tag{A.7}$$

Summing Eq. (A.7) with the diffusion potential term in (A.2), gives:

$$\phi(h) - \phi(0) = \frac{RT}{F}\ln\frac{c(h)}{c(0)}, \tag{A.8}$$

which, of course, could have been obtained straight from Eq. (A.4), as we have done. Hence, Eq. (A.8) includes, indeed, also the ohmic drop in the membrane.

References

[1] J. de Gyves, E.R. de San Miguel, Ind. Eng. Chem. Res. 38 (1999) 2182.
[2] H.J. Lee, P.O. Beattie, B.J. Seddon, M.D. Osborne, H.H. Girault, J. Electroanal. Chem. 440 (1997) 73.
[3] W.J. Albery, J.F. Burke, E.B. Leffler, J. Hadgraft, J. Chem. Soc. Faraday Trans. I. 72 (1976) 1618.
[4] J.A. Manzanares, R.M. Lahtinen, B. Quinn, K. Kontturi, D.J. Schiffrin, Electrochim. Acta 44 (1998) 59.
[5] M.H. Barker, L. Murtomäki, K. Kontturi, J. Electroanal. Chem. 497 (2001) 61.
[6] Z. Samec, J. Langmaier, A. Trojánek, J. Electroanal. Chem. 426 (1997) 37.
[7] J. Hautojärvi, K. Kontturi, J.H. Näsman, B.L. Svarfvar, P. Viinikka, M. Vuoristo, Ind. Eng. Chem. Res. 35 (1996) 450.
[8] S. Åkerman, P. Viinikka, B.L. Svarfvar, K. Järvinen, K. Kontturi, J.H. Näsman, A. Urtti, P. Paronen, J. Contr. Rel. 50 (1998) 153.
[9] T. Kankkunen, R. Sulkava, M. Vuorio, K. Kontturi, J. Hirvonen, Pharm. Res. 19 (2002) 705.
[10] T. Kakiuchi, J. Electroanal. Chem. 322 (1992) 55.
[11] T. Kakiuchi, J. Noguchi, M. Senda, J. Electroanal. Chem. 336 (1992) 137.
[12] Z. Samec, T. Kakiuchi, M. Senda, Electrochim. Acta 40 (1995) 2971.
[13] V.G. Levich, Physicochemical Hydrodynamics, Prentice-Hall, Englewood Cliffs, NJ, 1962, p. 69.
[14] URL: http://www.ecochemie.nl/.
[15] URL: http://www.solartron.com/.
[16] Z. Samec, J. Langmayer, A. Trojánek, J. Electroanal. Chem. 409 (1996) 1.
[17] P.R. Brown, J.L. Hallman, L.W. Whaley, D.H. Desai, M.J. Pugia, R.A. Bartsch, J. Membr. Sci. 56 (1991) 195.
[18] A. Mälkiä, P. Liljeroth, A.K. Kontturi, K. Kontturi, J. Phys. Chem. B 105 (2001) 10884.
[19] O. Shirai, S. Kihara, Y. Yoshida, M. Matsui, J. Electroanal. Chem. 61 (1995) 61.
[20] C.M. Pereira, F. Silva, M.J. Sousa, K. Kontturi, L. Murtomäki, J. Electroanal. Chem. 509 (2001) 148.
[21] J.S. Newman, Electrochemical Systems, Prentice-Hall, Englewood Cliffs, NJ, 1973, p. 229.